Electronic Supplementary Material (ESI) for ChemComm.

Electronic Supplementary Information (ESI†)

A Cationic Sulfur-Hydrocarbon Triradical with an Excited Quartet State

Shuxuan Tang,[a] Huapeng Ruan,[a] Zhaobo Hu,[a] Yue Zhao,[a] You Song[a] and Xinping Wang*[a]

[a]State Key Laboratory of Coordination Chemistry, School of Chemistry and Chemical Engineering, Collaborative Innovation Center of Advanced Microstructures, Nanjing University, Nanjing 210023, China

*E-mail: xpwang@nju.edu.cn

Contents

General

All experiments were carried out under a nitrogen atmosphere by using standard Schlenk techniques and an argon-filled glovebox. Solvents were purified under the standard procedure. $ClCH_2CH_2Cl$ was distilled from CaH_2 and stored in molecular sieve. Dibutyl phthalate (DBP) was dried through molecular sieve. All of the solvents were degassed before using. Potassium carbonate was purchased and used upon arrival. 2,3,6,7,14,15-hexabromotriptycene, 1,2-benzenedithiol and $NO[Al(OR_F)_4]$ ($OR_F = OC(CF_3)_3$) were synthesized according to the reported procedures.[S1−S3] The ^1H NMR and ^{13}C NMR spectra were obtained with a Bruker Ultra Shield 400 MHz spectrometer using $(CD_3)_2SO$ as solvent and the data were listed in ppm referenced with internal standard Me_4Si. Single crystal X-ray diffraction was carried out by using a Bruker D8 CMOS detector. The structures were solved by direct methods and all refined on F^2 with the SHELX-2018 and Olex2 software package. The positions of the H atoms were calculated and considered isotropically according to a riding model. Cyclic voltammetry (CV) and differential pulse voltammetry (DPV) were performed on a CHI660E electrochemical workstation with platinum as the working and counter electrode, and Ag/AgCl electrode as reference. Freshly distilled $ClCH_2CH_2Cl$ was used as the solvent and *n*-Bu_4NPF_6 (10^{-1} M) was used as electrolyte. Continuous-wave EPR (CW-EPR) spectra were obtained using a Bruker EMX plus-6/1 variable-temperature apparatus and were simulated with the software of WINEPR SimFonia. The Zeeman splitting of **2a** was calculated using Easyspin on the basis of the simulation result.[S4] Pulse X-band EPR data were obtained on a CIQTEK EPR100 Spectrometer. Magnetic measurements were performed using a Quantum Design SQUID VSM magnetometer with a field of 0.1 T. UV−vis−NIR spectra were recorded on Lambda 750 spectrometer. Element analyses were performed at Shanghai Institute of Organic Chemistry, the Chinese Academy of Sciences.

Discussions on the oxidation reactions

It has to be noticed that we also carried out the oxidation reactions of **1** with other oxidants and solvents:

1. The reaction between **1** and $NOSbF_6$ in CH_2Cl_2 only resulted in insoluble dark blue powder with unreacted $NOSbF_6$ crystallite. This phenomenon is perhaps due to the low solubility of both $NOSbF_6$ and the radical product.
2. The reaction between **1** and $NOSbF_6$ in SO_2 (l) through a thick wall H-shaped Schlenk flask at room temperature resulted in insoluble dark blue powder. The $NOSbF_6$ features a relatively high solubility in SO_2 (l), which means that the finally insoluble powder might due to the low solubility of the radical product.
3. The reaction between **1** and $NO[Al(OR_F)_4]$ in CH_2Cl_2 first resulted in dark blue solution, then insoluble dark blue powder quickly formed. This phenomenon is perhaps due to the reactions between the radical product and the CH_2Cl_2 solvent molecule.

In summary, taken the solubility of both oxidant and product into consideration, the oxidant $NO[Al(OR_F)_4]$ was finally selected. Considering that CH_2Cl_2 solvent molecule may react with the radical product, $ClCH_2CH_2Cl$ was finally used, in view of both solubility and stability of the radical product.

Discussions on the solvent of frozen-solution CW-EPR measurements

The frozen-solution CW-EPR measurements of **2a** and **2b** were also carried out using $ClCH_2CH_2Cl$ as the solvent. However, zero-field splitting was not observed, which was probably due to the relatively high polarity of $ClCH_2CH_2Cl$.

DBP was finally used as the solvent in CW-EPR measurements, which features a relatively low polarity and acceptable solubility of **2a** and **2b**.

Synthesis of 1: A mixture of 2,3,6,7,14,15-hexabromotriptycene (364 mg, 0.5 mmol), 1,2-benzenedithiol (426 mg, 3.0 mmol) and potassium carbonate (414 mg, 3.0 mmol) in DMF (30 mL) was refluxed (150 °C) for 12 h under N_2 protection. After cooled down to room temperature and addition of methanol (50 mL), the mixture was stirred for 10 min and then filtered. The residue was purified by chromatography on silica gel using petroleum ether/chloroform = 1/2 as eluent. The compound **1** was obtained as white solid. The crystals suitable for single-crystal X-ray diffraction were obtained by slowly evaporating a saturated mixture solvent (petroleum ether/chloroform = 1/2) solution of **1**. Yield: 0.180 g, 54%. ^{1}H NMR (400 MHz, $(CD_3)_2SO$, ppm): δ 7.55 (s, 6 H, phenyl-H), 7.53 (m, 6 H, phenyl-H), 7.30 (m, 6 H, phenyl-H), 5.54 (s, 2 H, CH); ^{13}C NMR (100.61 MHz, $(CD_3)_2SO$, ppm): δ 144.44, 134.56, 131.39, 128.69, 128.19, 124.23, 50.34.

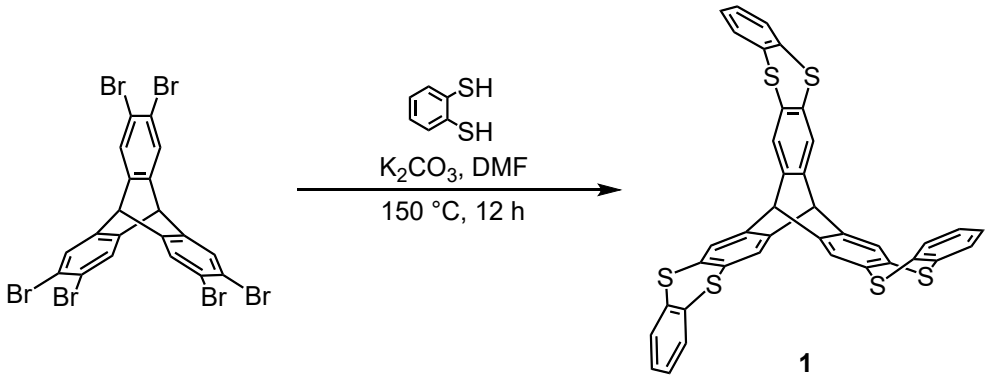

Scheme S1 Synthesis of **1**.

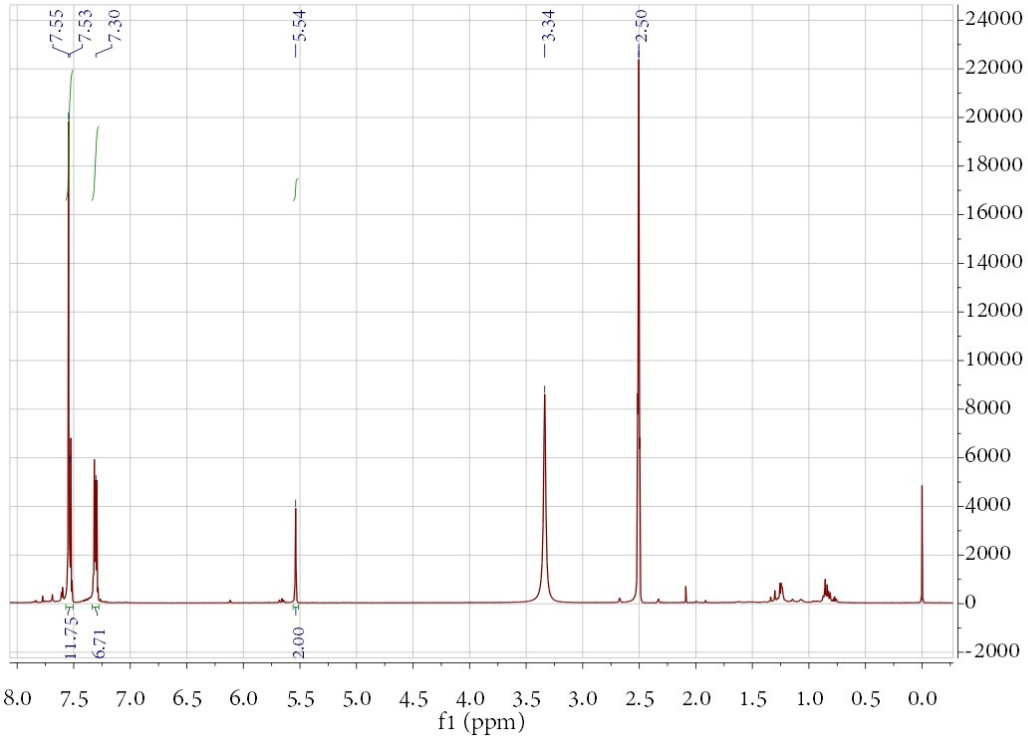

Fig. S1 ^{1}H NMR spectrum of **1** in $(CD_3)_2SO$.

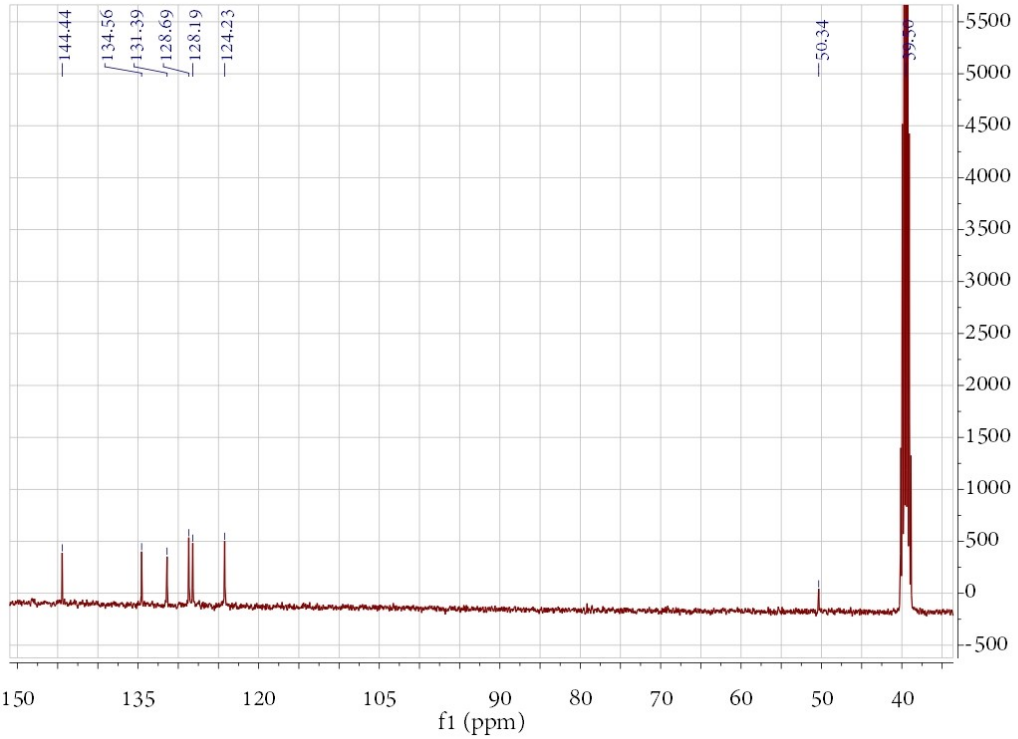

Fig. S2 ^{13}C NMR spectrum of **1** in $(CD_3)_2SO$.

Synthesis of 2a: Under anaerobic and anhydrous condition, solution of $NO[Al(OR_F)_4]$ (152 mg, 0.152 mmol) in $ClCH_2CH_2Cl$ (20 mL) was added dropwise to a suspension of **1** (33 mg, 0.050 mmol) in $ClCH_2CH_2Cl$ (30 mL). The reaction mixture was stirred at room temperature for 12 h. The resultant dark purple mixture was filtered and the filtrate was then concentrated and left in a –35 ℃ fridge for 12 h to form dark blue crystals of **2a**. Yield: 0.031 g, 17%. Elemental analysis for $C_{88}H_{24}Al_3Cl_2F_{108}O_{12}S_6$ (%), cacld: C 28.81; H 0.66; found: C 28.93; H 0.70.

Synthesis of 2b: The synthesis procedure of **2b** is similar to that of **2a**. Under anaerobic and anhydrous condition, solution of $NO[Al(OR_F)_4]$ (152 mg, 0.152 mmol) in $ClCH_2CH_2Cl$ (20 mL) was added dropwise to a suspension of **1** (33 mg, 0.050 mmol) in $ClCH_2CH_2Cl$ (30 mL). The reaction mixture was stirred at room temperature for 12 h. The resultant dark purple mixture was filtered and the filtrate was then concentrated and left at room temperature for 2 days to form dark blue crystals of **2b**. Yield: 0.039 g, 21%. Elemental analysis for $C_{86}H_{20}Al_3F_{108}O_{12}S_6$ (%), cacld: C 28.93; H 0.56; found: C 29.11; H 0.62.

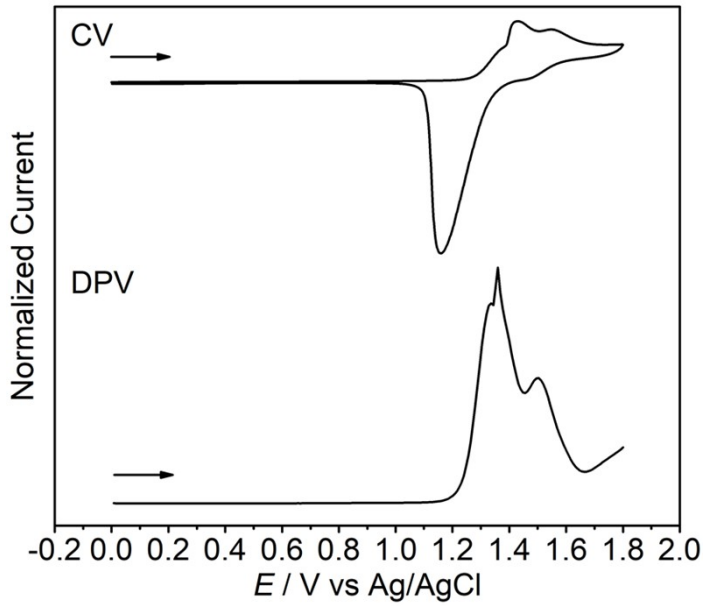

Fig. S3 Cyclic voltammetry (CV) and differential pulse voltammetry (DPV) of **1**.

Table S1 Crystal Data and Structure Refinement for **1**, **2a**, and **2b**

	1	**2a**	**2b**
Empirical formula	$C_{38}H_{20}S_6$	$C_{88}H_{24}Al_3Cl_2F_{108}O_{12}S_6$	$C_{86}H_{20}Al_3F_{108}O_{12}S_6$
Formula weight (g mol^{-1})	668.90	3669.27	3570.32
Crystal system	hexagonal	triclinic	monoclinic
Space group	$P6_3/m$	$P\bar{1}$	$P2_1/c$
Z	2	2	4
Temperature (K)	193	193	193
μ (mm^{-1})	0.482	0.400	2.132
a (Å)	12.143(3)	12.318(2)	27.8747(14)
b (Å)	12.143(3)	17.946(3)	20.9396(11)
c (Å)	11.827(4)	27.986(5)	21.1968(11)
α (°)	90	88.353(5)	90
β (°)	90	88.861(5)	95.191(3)
γ (°)	120	81.464(5)	90
Volume (Å^3)	1510.2(9)	6114.6(18)	12321.5(11)
R_1 [I > 2σ (I)]	0.1345	0.0839	0.1179
wR_2 [all data]	0.2978	0.2620	0.2583

Table S2 Selected Bond Distances (Å)

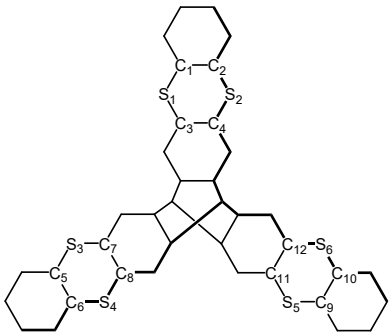

	1	**2a**	**2b**
S_1–C_1	1.769(10)	1.719(5)	1.712(8)
S_1–C_3	1.801(8)	1.721(4)	1.724(7)
S_2–C_2	1.769(10)	1.727(5)	1.707(8)
S_2–C_4	1.801(8)	1.715(4)	1.726(7)
S_3–C_5	1.769(10)	1.724(5)	1.715(7)
S_3–C_7	1.801(8)	1.718(5)	1.725(6)
S_4–C_6	1.769(10)	1.721(5)	1.710(6)
S_4–C_8	1.801(8)	1.727(4)	1.724(6)
S_5–C_9	1.769(10)	1.714(5)	1.714(7)
S_5–C_{11}	1.801(8)	1.714(5)	1.716(6)
S_6–C_{10}	1.769(10)	1.733(5)	1.723(6)
S_6–C_{12}	1.801(8)	1.726(5)	1.714(6)

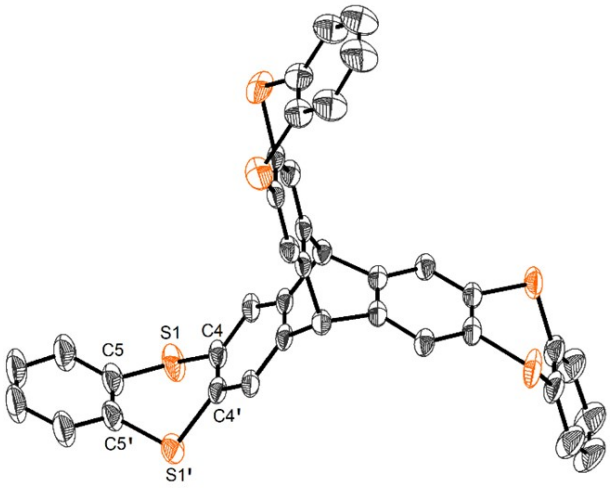

Fig. S4 Thermal ellipsoid (30%) drawing of **1**. All hydrogen atoms are not shown for clarity. Selected bond lengths (Å) and bond angles (°): S1–C4 1.801(8), S1–C5 1.769(10), C4–C4' 1.35(2), C5–C5' 1.35(2), C5–S1–C4 98.6(4), S1–C4–C4' 121.0(3), S1–C5–C5' 121.5(4).

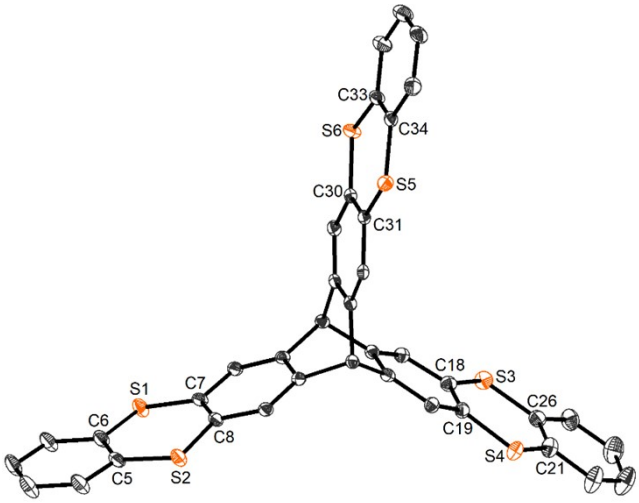

Fig. S5 Thermal ellipsoid (30%) drawing of the trication part for **2a**. All hydrogen atoms are not shown for clarity. Selected bond lengths (Å) and bond angles (°): S1–C6 1.724(5), S1–C7 1.718(5), S2–C5 1.721(5), S2–C8 1.727(4), C5–C6 1.411(7), C7–C8 1.400(6), S3–C18 1.714(5), S3–C26 1.714(5), S4–C19 1.726(5), S4–C21 1.733(5), C18–C19 1.407(7), C21–C26 1.385(8), S5–C31 1.715(4), S5–C34 1.727(5), S6–C30 1.721(4), S6–C33 1.719(5), C30–C31 1.408(6), C33–C34 1.394(7), C6–S1–C7 107.2(2), C5–S2–C8 107.8(2), S1–C6–C5 126.1(4), S1–C7–C8 126.8(4), S2–C5–C6 125.7(4), S2–C8–C7 125.5(3), C18–S3–C26 107.4(2), C19–S4–C21 106.9(2), S3–C18–C19 126.9(4), S3–C26–C21 126.1(4), S4–C19–C18 125.3(3), S4–C21–C26 127.0(4), C31–S5–C34 107.5(2), C30–S6–C33 107.3(2), S5–C31–C30 125.5(3), S5–C34–C33 126.6(4), S6–C30–C31 126.8(3), S6–C33–C34 126.0(4).

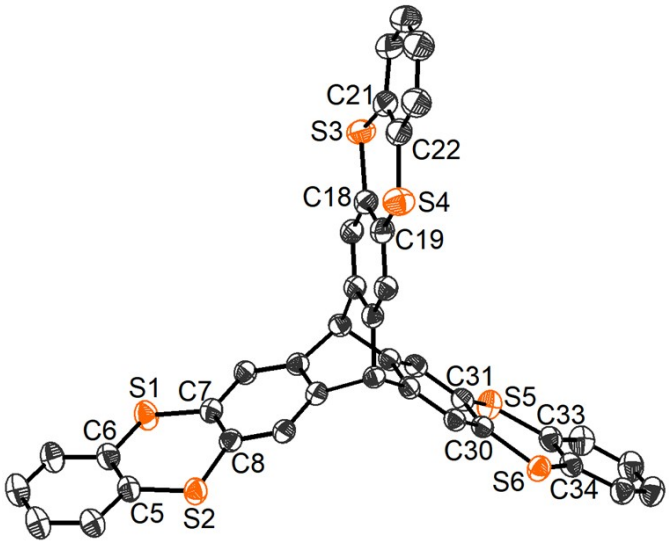

Fig. S6 Thermal ellipsoid (30%) drawing of the trication part for **2b**. All hydrogen atoms are not shown for clarity. Selected bond lengths (Å) and bond angles (°): S1–C6 1.715(7), S1–C7 1.725(6), S2–C5 1.710(6), S2–C8 1.724(6), C5–C6 1.398(9), C7–C8 1.399(8), S3–C18 1.724(7), S3–C21 1.712(8), S4–C19 1.726(7), S4–C22 1.707(8), C18–C19 1.400(9), C21–C22 1.410(11), S5–C31 1.716(6), S5–C33 1.714(7), S6–C30 1.714(6), S6–C34 1.723(6), C30–C31 1.419(8), C33–C34 1.402(9), C6–S1–C7 107.5(3), C5–S2–C8 107.1(3), S1–C6–C5 125.8(5), S1–C7–C8 125.4(5), S2–C5–C6 126.4(5), S2–C8–C7 126.2(5), C18–S3–C21 107.4(4), C19–S4–C22 107.7(4), S3–C18–C19 126.1(5), S3–C21–C22 126.1(6), S4–C19–C18 125.9(5), S4–C22–C21 126.1(6), C31–S5–C33 107.4(3), C30–S6–C34 107.3(3), S5–C31–C30 125.9(5), S5–C33–C34 126.2(5), S6–C30–C31 125.9(5), S6–C34–C33 126.1(5).

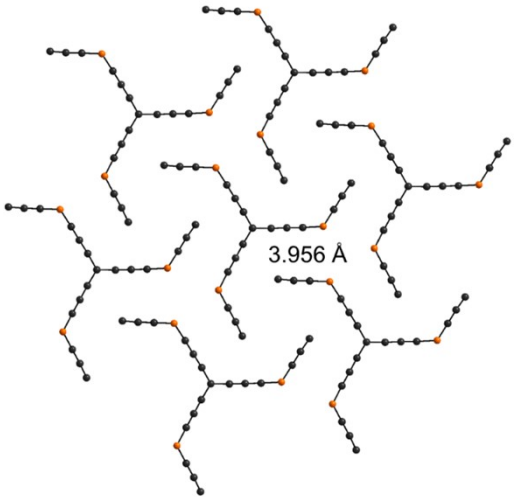

Fig. S7 Crystal packing of **1**.

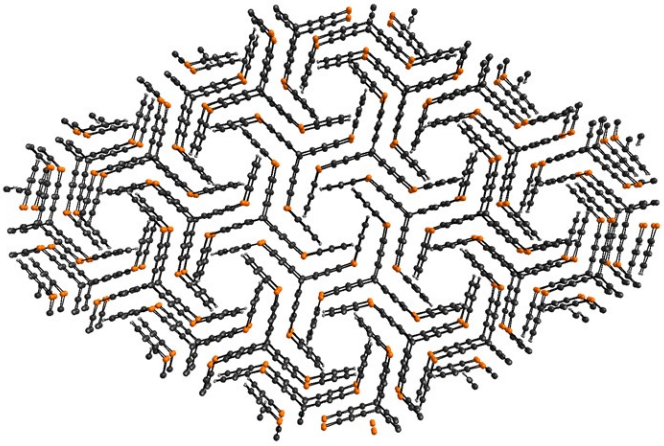

Fig. S8 The one-dimensional pore passages in the crystal structure of **1**.

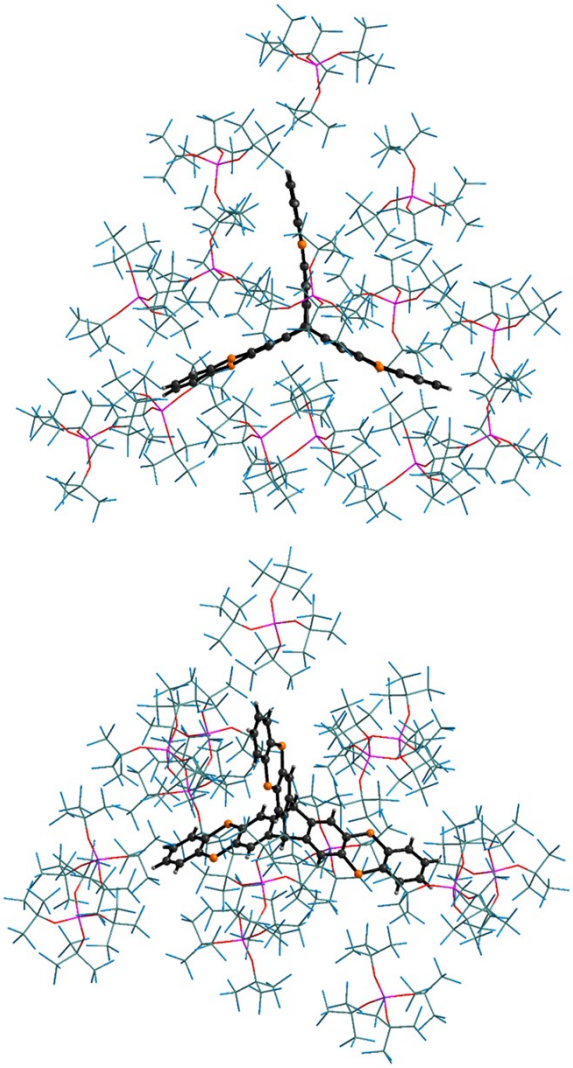

Fig. S9 Crystal packing of **2a**.

Continuous-Wave EPR Measurements and Simulation

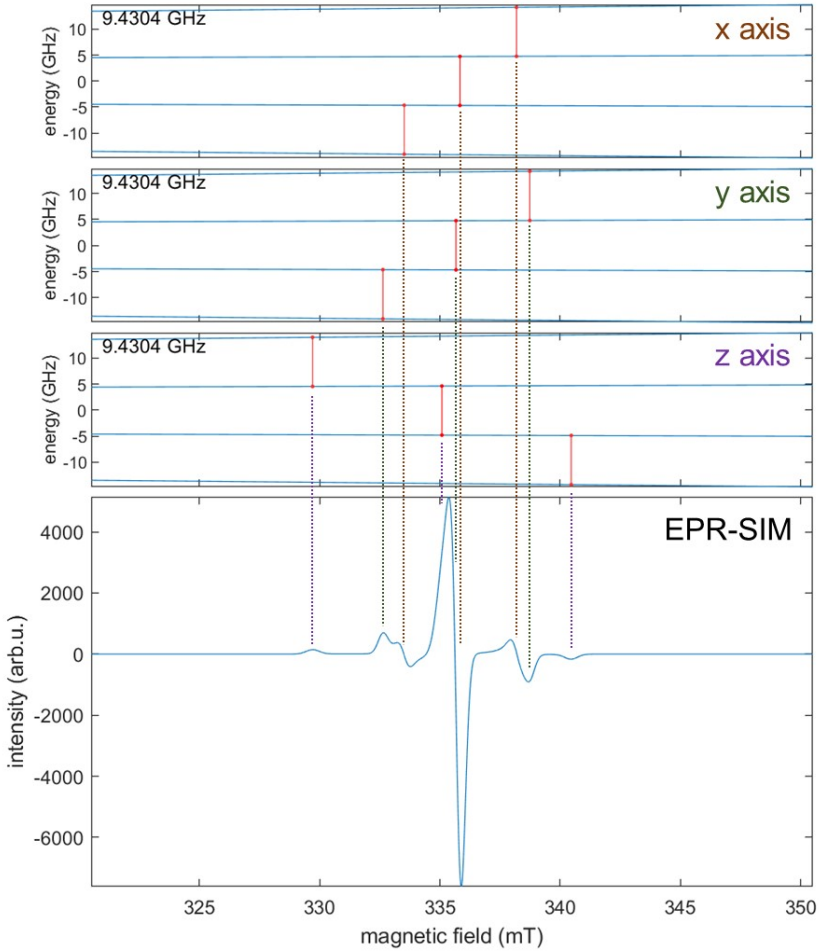

Fig. S10 Calculated Zeeman splitting and allowed transitions ($\Delta m_s = \pm 1$) at x, y, and z axis for **2a**.

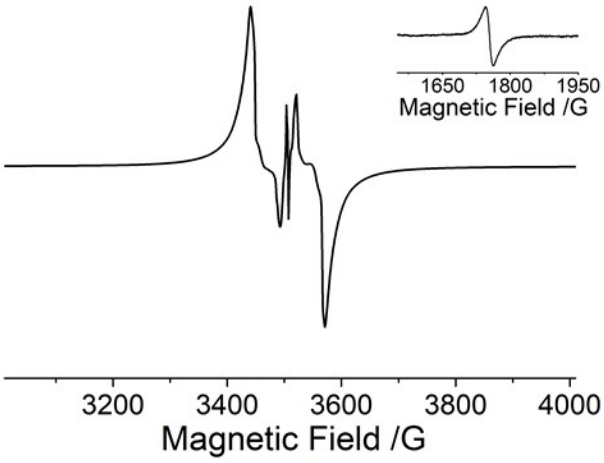

Fig. S11 The EPR spectrum of **2a** powder at room temperature (v = 9.8526 GHz).

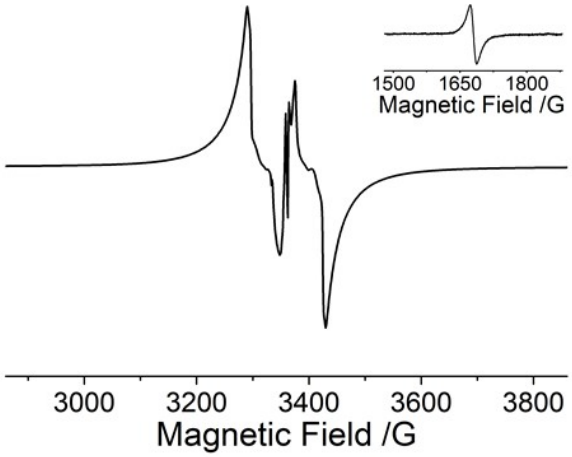

Fig. S12 The EPR spectrum of **2a** powder at 88 K (v = 9.4395 GHz).

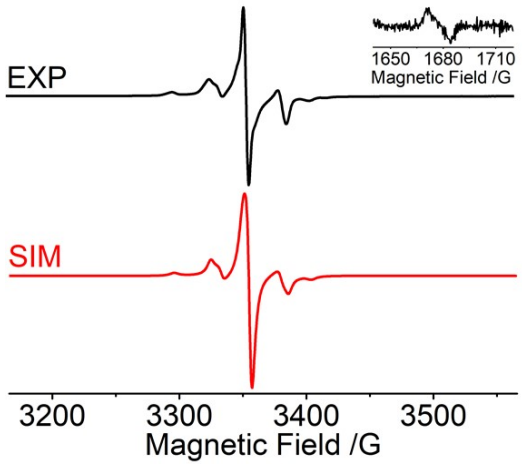

Fig. S13 Frozen-solution EPR spectrum of 1×10^{-4} M **2b** in dibutyl phthalate (DBP) at 88 K (EXP, v = 9.4263 GHz) and the simulated spectrum (SIM). The zero-field splitting (ZFS) parameters were simulated as D = 27.0 G and E = 1.2 G. The anisotropic g factors were simulated as g_x = 2.0065, g_y = 2.0072, and g_z = 2.0105.

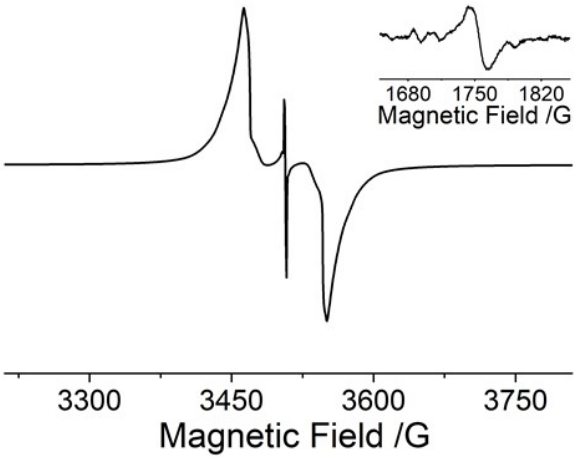

Fig. S14 The EPR spectrum of **2b** powder at room temperature (v = 9.8565 GHz).

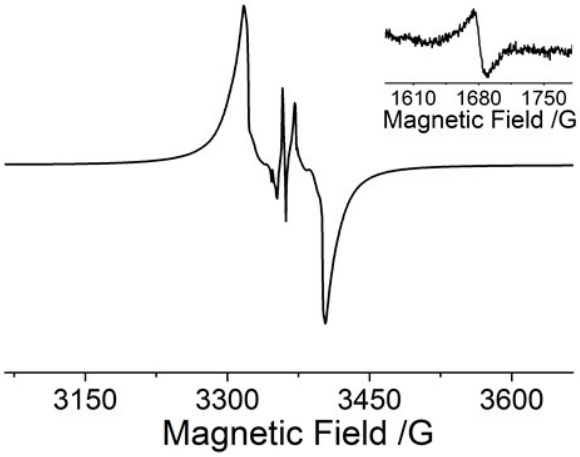

Fig. S15 The EPR spectrum of **2b** powder at 88 K (v = 9.4443 GHz).

Pulse EPR Measurements

Pulse X-band EPR data were obtained on a CIQTEK EPR100 Spectrometer. The measurements were performed on the powder sample of **2a**.[S5]

T_1 values were measured using a three-pulse inversion recovery sequence (π–T–$\pi/2$–τ–π–τ–echo) with τ of 400 ns. T_2 values were collected using a two-pulse echo sequence ($\pi/2$–τ–π–τ–echo). The $\pi/2$ and π pulses were set to be 16 ns and 32 ns, respectively. Both T_1 and T_2 were measured in the temperature range from 6 K to 30 K, and fitted by a single exponent function $y = y_0 + A*\exp(-x/T)$.

Field-swept electron spin echo-detected (FSED) EPR spectrum was recorded using a two-pulse echo sequence ($\pi/2$–τ–π–τ–echo) with microwave pulse lengths of 16 ns and 32 ns, and an interpulse delay τ = 400 ns.

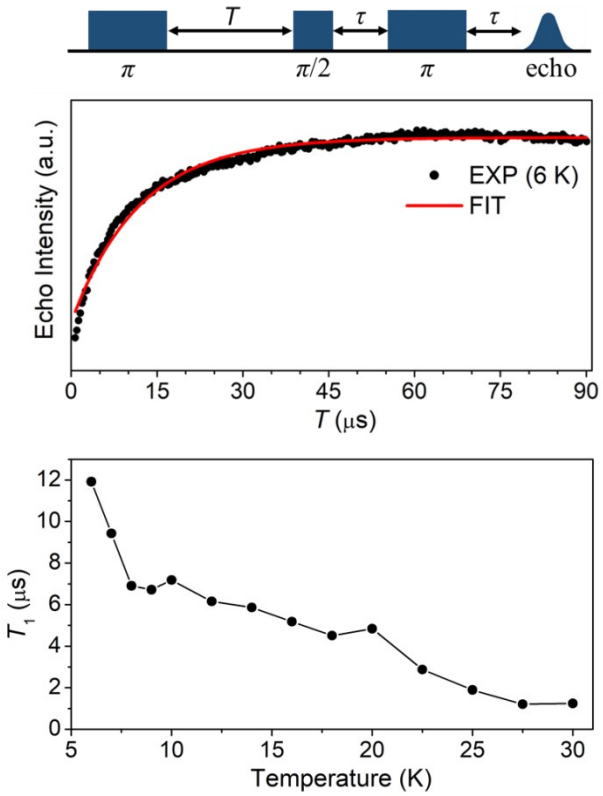

Fig. S16 Top: The three-pulse inversion recovery sequence applied to **2a**.
Middle: Echo intensity for **2a** as a function of wait time T at 6 K. The red line indicates the best fit of the recovery curve, which yields T_1 = 11.92 μs.
Bottom: Spin-lattice relaxation times (T_1) as a function of temperature for **2a**.

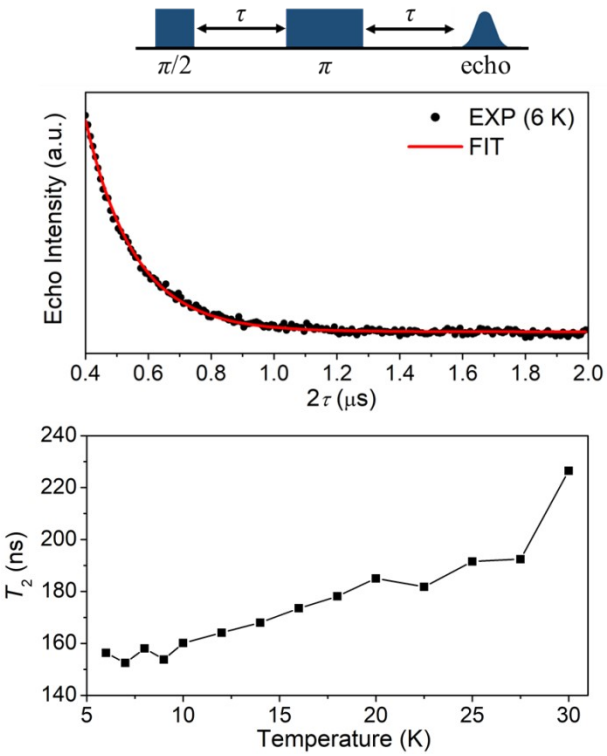

Fig. S17 Top: The two-pulse echo sequence applied to **2a**.
Middle: Echo intensity for **2a** as a function of interpulse spacing 2τ at 6 K. The red line indicates the best fit of the decay curve, which yields T_2 = 156.4 ns.
Bottom: Coherence times (T_2) as a function of temperature for **2a**.

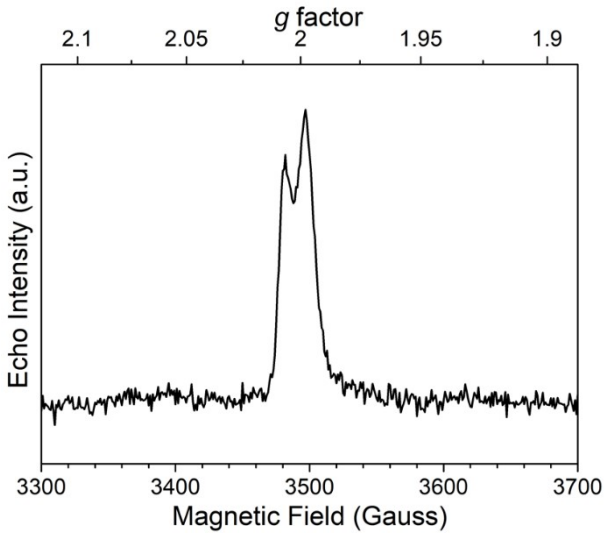

Fig. S18 FSED EPR spectrum of **2a** at 6 K.

Table S3 Variable-Temperature Inversion Recovery Curves for **2a**. Red lines are best fits of the recovery curves.

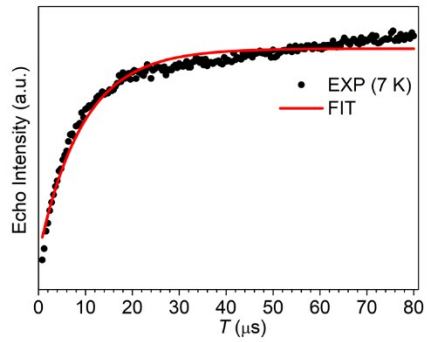	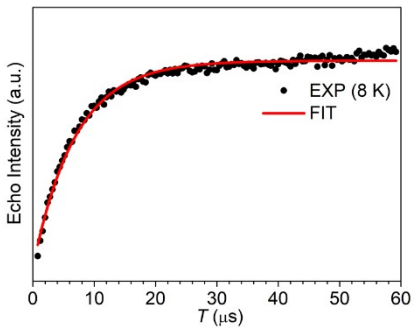	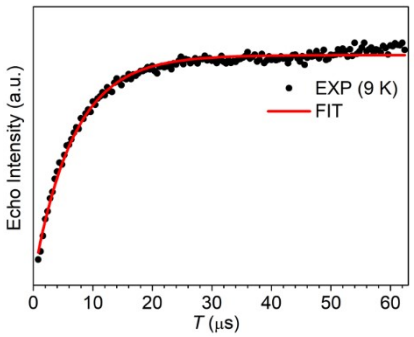
7 K	8 K	9 K
T_1 = 9.427 μs	T_1 = 6.906 μs	T_1 = 6.719 μs
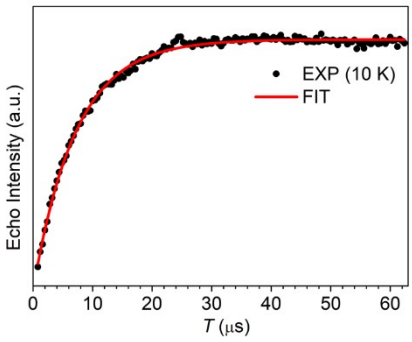	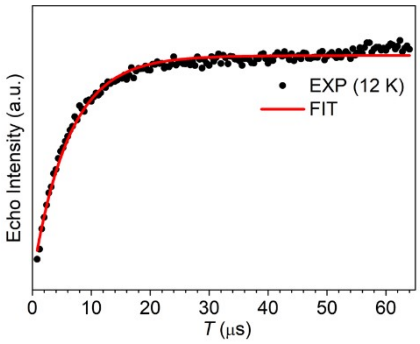	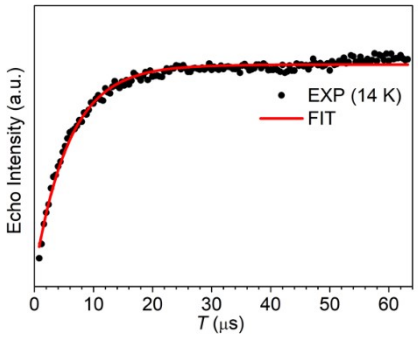
10 K	12 K	14 K
T_1 = 7.184 μs	T_1 = 6.154 μs	T_1 = 5.863 μs
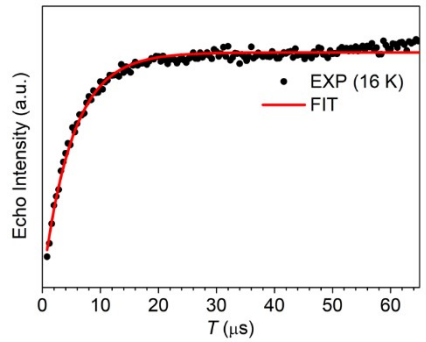	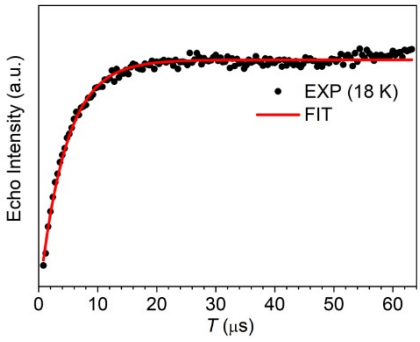	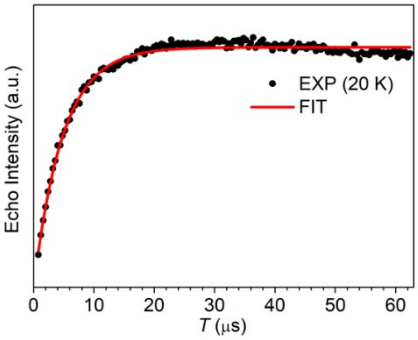
16 K	18 K	20 K
T_1 = 5.183 μs	T_1 = 4.510 μs	T_1 = 4.840 μs
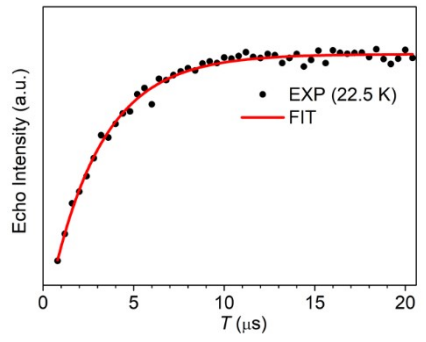	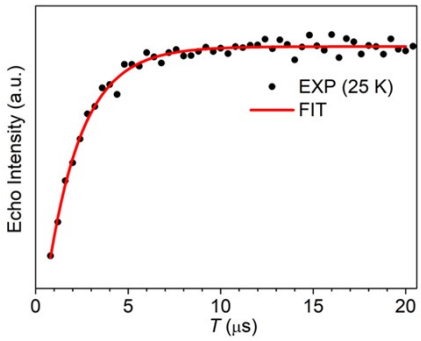	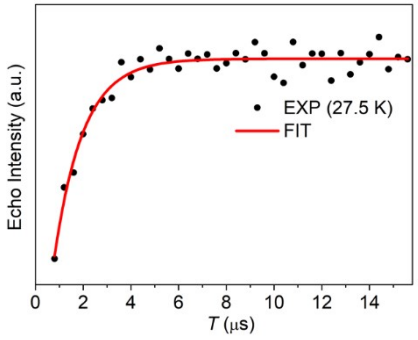
22.5 K	25 K	27.5 K
T_1 = 2.872 μs	T_1 = 1.892 μs	T_1 = 1.208 μs

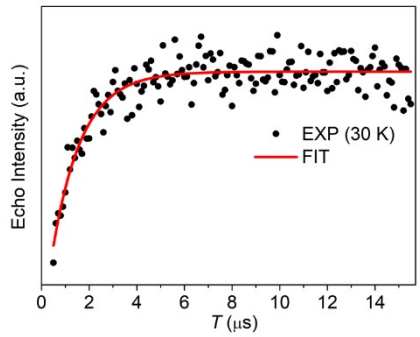		
30 K		
T_1 = 1.246 μs		

Table S4 Variable-Temperature Echo-Decay Curves for **2a**. Red lines are best fits of the decay curves.

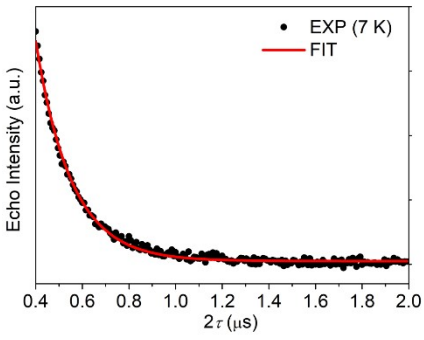	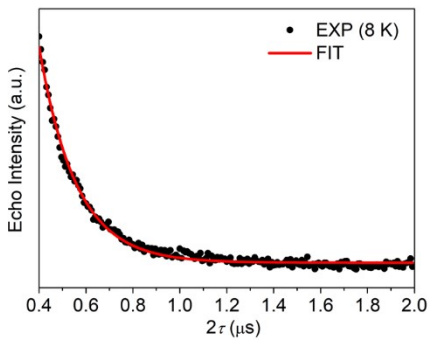	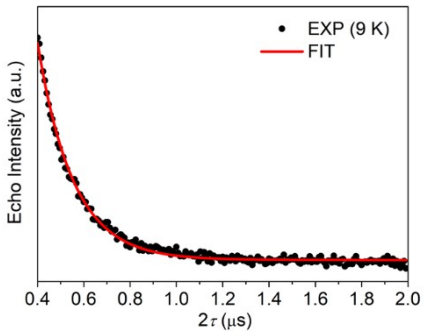
7 K	8 K	9 K
T_2 = 152.5 ns	T_2 = 158.1 ns	T_2 = 153.8 ns
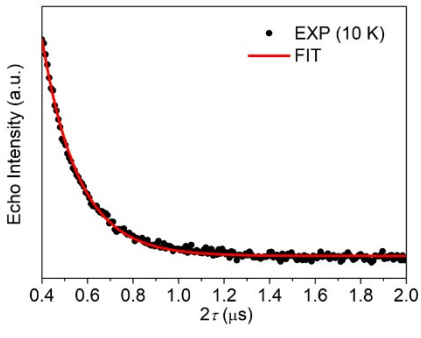	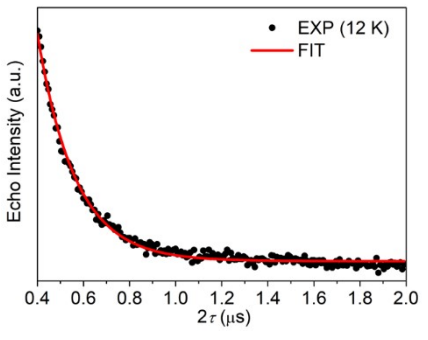	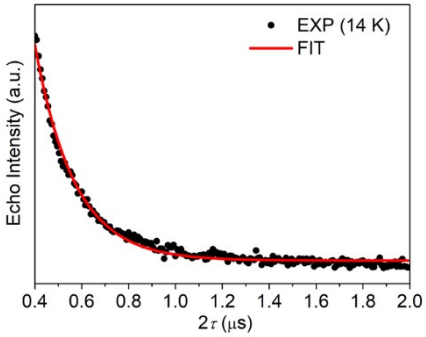
10 K	12 K	14 K
T_2 = 160.2 ns	T_2 = 164.2 ns	T_2 = 168.0 ns
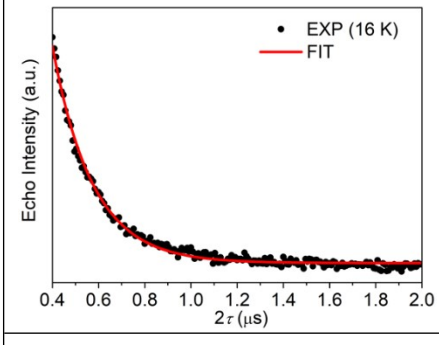	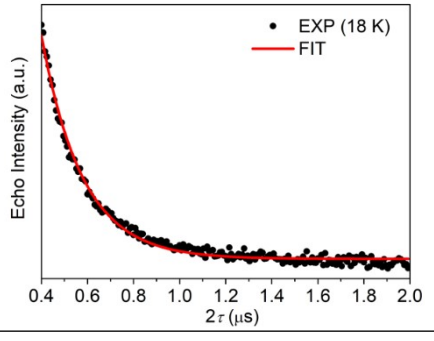	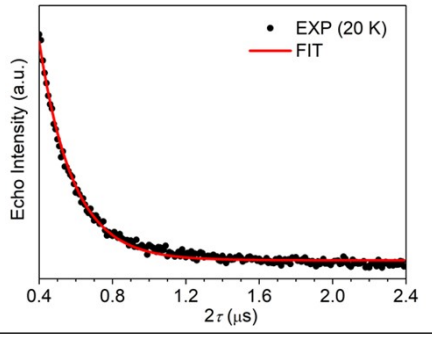
16 K	18 K	20 K

T_2 = 173.5 ns	T_2 = 178.1 ns	T_2 = 185.0 ns
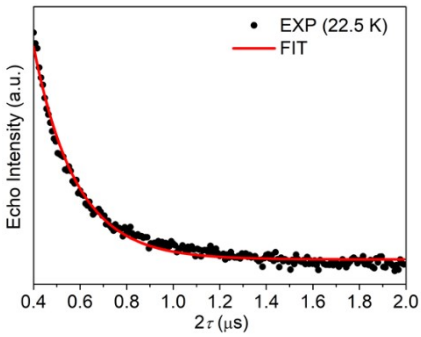	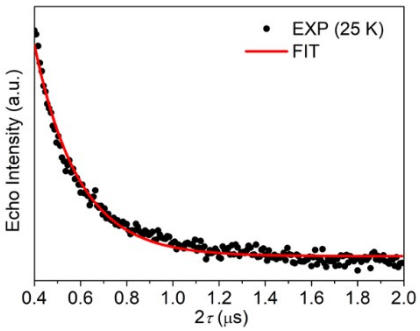	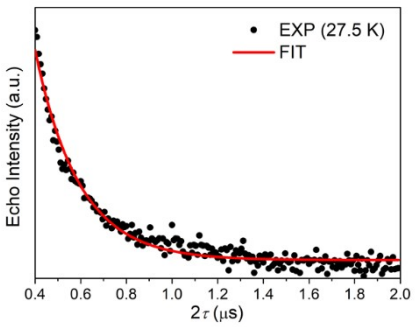
22.5 K	25 K	27.5 K
T_2 = 181.8 ns	T_2 = 191.6 ns	T_2 = 192.4 ns
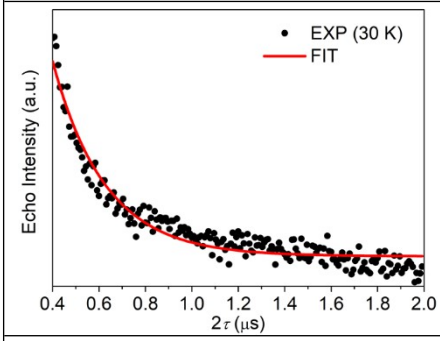		
30 K		
T_2 = 226.5 ns		

SQUID Measurements

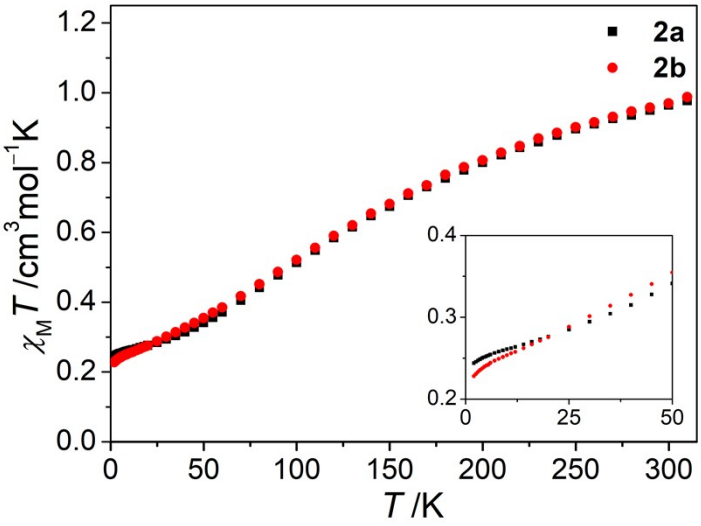

Fig. S19 Comparison between the $\chi_M T$ versus T curves for **2a** and **2b**.

DFT Calculations

All calculations were carried out at the Gaussian 09 program.[S6] The geometric optimizations of the studied compounds were obtained at the (U)PBE0/6-311G* level of theory. The obtained stationary points were characterized by frequency calculations. For the doublet state of the triradical trication in **2a** and **2b**, the symmetry-broken approaches were carried out ($\langle S^2 \rangle$ = 1.75). The spin contamination errors were corrected by the approximate spin-projection (AP) method when evaluating the energy gap.[S7] The energy data are listed in Table S5. The calculated bond distances are listed in Table S6. The calculated Mulliken population are listed in Table S7. Although the triradical trication in **2a** and **2b** possesses two doublet states and one quartet state, only one doublet state and one quartet state were selected for structural optimization to save computation time. The calculated doublet-quartet energy gap is obtained with ΔE = –192.4 cm^{-1} (–550.0 cal mol^{-1}).

Table S5 Energy Data of DFT Calculations

	Annihilation of the first spin contaminant ($\langle S^2 \rangle$)	Sum of electronic and zero-point Energies (eV)	ΔE_{Q-D} before correction (kcal mol^{-1})	ΔE_{Q-D} after correction (kcal mol^{-1})
Doublet	1.7541	–3845.639549	0	0
Quartet	3.7724	–3845.639080	0.29430219	0.550079563

$$E_{AP} = \alpha E_D - \beta E_Q$$

$$\alpha = \frac{\langle S^2 \rangle_Q}{\langle S^2 \rangle_Q - \langle S^2 \rangle_D}$$

$$\beta = \alpha - 1 = \frac{\langle S^2 \rangle_D}{\langle S^2 \rangle_Q - \langle S^2 \rangle_D}$$

$$\Delta E_{Q-D} = E_Q - E_{AP}$$

Table S6 Calculated Bond Distances (Å) of the Sulfur-Hydrocarbons for **1** and the Triradical Trication in **2a** and **2b**

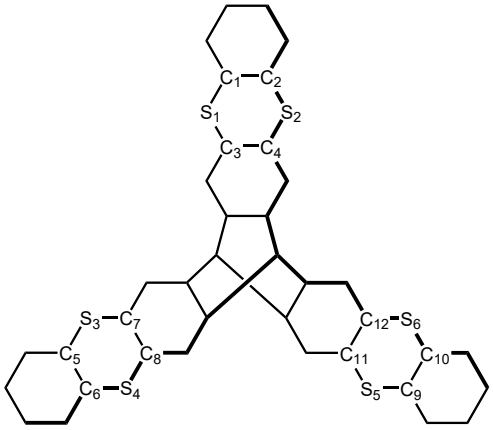

	1	triradical trication-doublet state	triradical trication-quartet state
S_1–C_1	1.77184	1.73070	1.73037
S_1–C_3	1.77093	1.73241	1.73319
S_2–C_2	1.77184	1.73070	1.73037
S_2–C_4	1.77093	1.73241	1.73319
S_3–C_5	1.77157	1.73044	1.73039
S_3–C_7	1.77091	1.73278	1.73324
S_4–C_6	1.77157	1.73044	1.73039
S_4–C_8	1.77091	1.73278	1.73324
S_5–C_9	1.77177	1.73057	1.73035
S_5–C_{11}	1.77085	1.73255	1.73321
S_6–C_{10}	1.77177	1.73057	1.73035
S_6–C_{12}	1.77085	1.73255	1.73322

Table S7 Calculated Mulliken Population of the Triradical Trication

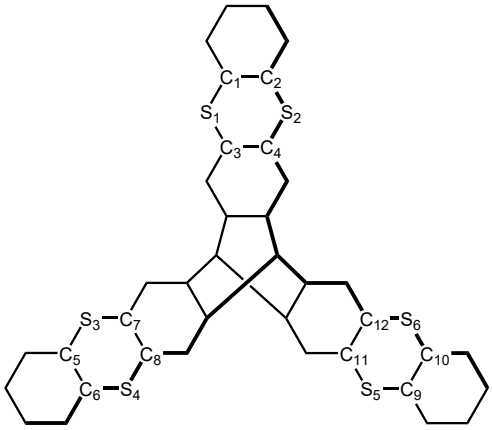

	triradical trication-doublet state	triradical trication-quartet state
S_1	–0.30136	0.30410
S_2	–0.30136	0.30410
C_1	–0.09623	0.09807
C_2	–0.09623	0.09807
C_3	–0.04688	0.04861
C_4	–0.04688	0.04861
S_3	0.30274	0.30413
S_4	0.30274	0.30413
C_5	0.09738	0.09812
C_6	0.09738	0.09812
C_7	0.04741	0.04855
C_8	0.04741	0.04855
S_5	0.30271	0.30409
S_5	0.30272	0.30409
C_9	0.09722	0.09810
C_{10}	0.09722	0.09810
C_{11}	0.04749	0.04857
C_{12}	0.04749	0.04857

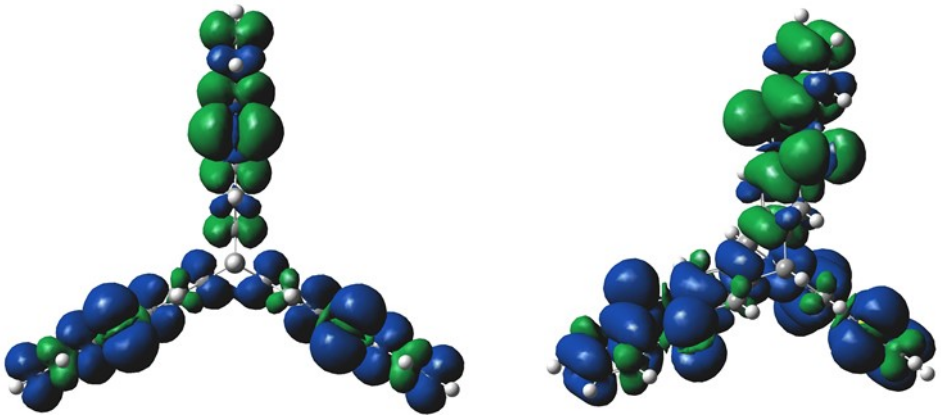

Fig. S20 Calculated spin density distribution of the triradical trication in the doublet state. Isovalue = 0.0004.

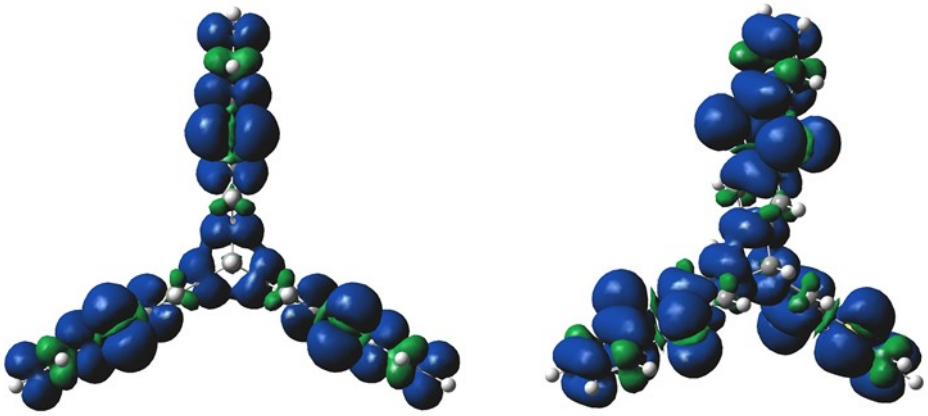

Fig. S21 Calculated spin density distribution of the triradical trication in the quartet state. Isovalue = 0.0004.

Coordinates of the studied molecules

Neutral compound 1

S	-1.508852000	5.109951000	1.598895000	S	-1.508852000	5.109951000	-1.598895000
C	-0.378149000	1.353155000	0.699545000	C	-0.378149000	1.353155000	-0.699545000
C	-1.027041000	3.663693000	0.697576000	C	-1.027041000	3.663693000	-0.697576000
C	-0.000124000	0.006817000	1.293371000	C	-0.000124000	0.006817000	-1.293371000
H	-0.000193000	0.006968000	2.384635000	H	-0.000193000	0.006968000	-2.384635000
C	-0.677425000	2.505785000	1.398894000	C	-0.677425000	2.505785000	-1.398894000
H	-0.652383000	2.523280000	2.484435000	H	-0.652383000	2.523280000	-2.484435000
C	-0.636950000	6.362377000	0.698547000	C	-0.636950000	6.362377000	-0.698547000
C	0.018894000	7.377796000	1.390895000	C	0.018894000	7.377796000	-1.390895000
H	0.036974000	7.356880000	2.475814000	H	0.036974000	7.356880000	-2.475814000
C	0.633555000	8.409876000	0.695188000	C	0.633555000	8.409876000	-0.695188000
H	1.127738000	9.206575000	1.241805000	H	1.127738000	9.206575000	-1.241805000
S	5.171857000	-1.248086000	1.598368000	S	5.171857000	-1.248086000	-1.598368000
C	1.355317000	-0.338456000	0.699683000	C	1.355317000	-0.338456000	-0.699683000
C	3.679378000	-0.936789000	0.697541000	C	3.679378000	-0.936789000	-0.697541000
C	2.502796000	-0.656928000	1.399046000	C	2.502796000	-0.656928000	-1.399046000
H	2.505181000	-0.688728000	2.484577000	H	2.505181000	-0.688728000	-2.484577000
C	5.812305000	-2.633466000	0.698526000	C	5.812305000	-2.633466000	-0.698526000
C	6.355867000	-3.713269000	1.390938000	C	6.355867000	-3.713269000	-1.390938000
H	6.328494000	-3.718477000	2.475849000	H	6.328494000	-3.718477000	-2.475849000
C	6.933704000	-4.766440000	0.695145000	C	6.933704000	-4.766440000	-0.695145000
H	7.370271000	-5.596146000	1.241741000	H	7.370271000	-5.596146000	-1.241741000
S	-3.655015000	-3.860926000	1.598425000	S	-3.655015000	-3.860926000	-1.598425000
C	-0.975641000	-0.994880000	0.699526000	C	-0.975641000	-0.994880000	-0.699526000
C	-2.647293000	-2.716856000	0.697478000	C	-2.647293000	-2.716856000	-0.697478000
C	-1.821474000	-1.833298000	1.398932000	C	-1.821474000	-1.833298000	-1.398932000
H	-1.850307000	-1.819935000	2.484470000	H	-1.850307000	-1.819935000	-2.484470000
C	-5.175956000	-3.737285000	0.698467000	C	-5.175956000	-3.737285000	-0.698467000
C	-6.383407000	-3.681174000	1.390968000	C	-6.383407000	-3.681174000	-1.390968000
H	-6.374176000	-3.653711000	2.475881000	H	-6.374176000	-3.653711000	-2.475881000
C	-7.584622000	-3.668897000	0.695169000	C	-7.584622000	-3.668897000	-0.695169000
H	-8.521848000	-3.642292000	1.241707000	H	-8.521848000	-3.642292000	-1.241707000

Triradical trication - doublet state

S	-5.043221000	-1.316548000	1.722492000	C	2.677381000	-2.704389000	0.703779000
S	-5.042994000	-1.316528000	-1.723164000	C	-1.356430000	-0.357560000	-0.705586000
S	3.666911000	-3.696341000	1.722897000	C	1.813006000	-1.835656000	1.401460000
S	3.667133000	-3.696302000	-1.722493000	H	1.817565000	-1.840760000	2.487779000
S	1.379228000	5.015296000	1.722892000	C	0.979449000	-0.996986000	-0.705425000
S	1.379451000	5.015325000	-1.722622000	C	-3.686970000	-0.963829000	0.703329000
C	0.365617000	1.343594000	0.705558000	C	-0.004435000	-0.004326000	1.302354000
C	1.813187000	-1.835627000	-1.401255000	H	-0.004437000	-0.004374000	2.392356000
H	1.817885000	-1.840709000	-2.487574000	C	-0.004268000	-0.004303000	-1.302348000
C	-2.500938000	-0.655302000	1.401198000	H	-0.004129000	-0.004332000	-2.392350000
H	-2.507565000	-0.657128000	2.487508000	C	1.005722000	3.664996000	0.703855000
C	0.679690000	2.483513000	1.401400000	C	-6.398794000	-1.670223000	0.706744000
H	0.681225000	2.490028000	2.487721000	C	1.005813000	3.665008000	-0.703656000
C	-2.500755000	-0.655281000	-1.401527000	C	4.652823000	-4.692128000	-0.706813000
H	-2.507240000	-0.657090000	-2.487838000	C	-6.398700000	-1.670215000	-0.707599000
C	0.365708000	1.343607000	-0.705481000	C	-7.580144000	-1.978282000	1.397877000
C	2.677472000	-2.704374000	-0.703481000	H	-7.584013000	-1.979303000	2.483480000
C	-3.686877000	-0.963820000	-0.703817000	C	-7.579957000	-1.978268000	-1.398893000
C	-1.356521000	-0.357572000	0.705412000	H	-7.583681000	-1.979279000	-2.484496000
C	0.679870000	2.483537000	-1.401263000	C	1.750173000	6.366659000	-0.706856000
H	0.681544000	2.490071000	-2.487584000	C	5.511916000	-5.559122000	1.398675000
C	0.979358000	-0.997000000	0.705540000	H	5.514483000	-5.562187000	2.484267000

C	-8.730109000	-2.278143000	0.701194000	C	6.348888000	-6.403160000	-0.701351000
H	-9.638639000	-2.515032000	1.243392000	H	7.009824000	-7.069949000	-1.243643000
C	4.652731000	-4.692144000	0.707321000	C	6.348797000	-6.403177000	0.702040000
C	5.512098000	-5.559089000	-1.398075000	H	7.009662000	-7.069978000	1.244401000
H	5.514805000	-5.562129000	-2.483668000	C	2.389504000	8.689553000	-0.701384000
C	2.074046000	7.543590000	-1.398100000	H	2.638644000	9.594718000	-1.243717000
H	2.075051000	7.547568000	-2.483697000	C	2.073864000	7.543567000	1.398501000
C	1.750081000	6.366647000	0.707196000	H	2.074728000	7.547527000	2.484099000
C	-8.730016000	-2.278136000	-0.702367000	C	2.389412000	8.689542000	0.701845000
H	-9.638472000	-2.515020000	-1.244688000	H	2.638482000	9.594698000	1.244225000

Triradical trication - quartet state

S	1.734558000	4.897623000	1.722703000	C	2.468232000	-2.894066000	0.703358000
S	1.734464000	4.897415000	-1.723387000	C	2.221367000	6.211112000	0.706857000
S	-5.134252000	-0.952014000	1.723287000	C	2.468190000	-2.894151000	-0.703149000
S	-5.134348000	-0.952221000	-1.722884000	C	-6.514065000	-1.194527000	-0.707056000
S	3.382622000	-3.956184000	1.723080000	C	2.221329000	6.211026000	-0.707726000
S	3.382517000	-3.956394000	-1.722797000	C	2.643689000	7.356817000	1.397958000
C	0.896719000	-1.069590000	0.705427000	H	2.645175000	7.360526000	2.483611000
C	-2.550252000	-0.477969000	-1.401254000	C	2.643615000	7.356647000	-1.398988000
H	-2.557156000	-0.478801000	-2.487615000	H	2.645043000	7.360224000	-2.484642000
C	0.850112000	2.423691000	1.401159000	C	4.311161000	-5.005243000	-0.707100000
H	0.853232000	2.429946000	2.487525000	C	-7.716364000	-1.407030000	1.398772000
C	1.668215000	-1.965435000	1.401445000	H	-7.720232000	-1.407475000	2.484424000
H	1.673582000	-1.970021000	2.487803000	C	3.054908000	8.471844000	0.701235000
C	0.850034000	2.423522000	-1.401496000	H	3.379933000	9.352793000	1.243396000
H	0.853094000	2.429646000	-2.487863000	C	-6.514026000	-1.194441000	0.707565000
C	0.896679000	-1.069675000	-0.705347000	C	-7.716442000	-1.407199000	-1.398171000
C	-3.755862000	-0.699215000	-0.703133000	H	-7.720371000	-1.407775000	-2.483822000
C	1.262725000	3.577834000	-0.703521000	C	5.118467000	-5.921193000	-1.398332000
C	0.453014000	1.310080000	0.705289000	H	5.120962000	-5.924221000	-2.483979000
C	1.668133000	-1.965605000	-1.401302000	C	4.311206000	-5.005155000	0.707455000
H	1.673437000	-1.970321000	-2.487659000	C	3.054871000	8.471759000	-0.702423000
C	-1.387522000	-0.263673000	0.705494000	H	3.379867000	9.352641000	-1.244708000
C	-3.755822000	-0.699131000	0.703429000	C	-8.886738000	-1.614088000	-0.701503000
C	0.452975000	1.309995000	-0.705469000	H	-9.811390000	-1.777460000	-1.243690000
C	-2.550173000	-0.477801000	1.401456000	C	-8.886699000	-1.614003000	0.702195000
H	-2.557017000	-0.478505000	2.487818000	H	-9.811320000	-1.777310000	1.244454000
C	-1.387562000	-0.263757000	-0.705382000	C	5.904882000	-6.812254000	-0.701615000
C	1.262764000	3.577919000	0.703023000	H	6.526077000	-7.516425000	-1.243742000
C	-0.012848000	-0.007914000	1.302196000	C	5.118555000	-5.921019000	1.398750000
H	-0.012929000	-0.007926000	2.392309000	H	5.121119000	-5.923912000	2.484397000
C	-0.012921000	-0.008070000	-1.302193000	C	5.904927000	-6.812167000	0.702094000
H	-0.013064000	-0.008213000	-2.392305000	H	6.526157000	-7.516270000	1.244269000

References

S1 T.-Z. Xie, K. Guo, M. Huang, X. Lu, S.-Y. Liao, R. Sarkar, C. N. Moorefield, S. Z. D. Cheng, C. Wesdemiotis and G. R. Newkome, *Chem. –Eur. J.*, 2014, **20**, 11291–11294.

S2 D. M. Giolando and K. Kirschbaum, *Synthesis*, 1992, **5**, 451–452.

S3 A. Decken, H. D. B. Jenkins, G. B Nikiforov and J. Passmore, *Dalton Trans.*, 2004, 2496–2504.

S4 S. Stoll and A. Schweiger, *J. Magn. Reson.*, 2006, **178**, 42–55.

S5 References on pulse EPR measurements: (*a*) J. M. Zadrozny and D. E. Freedman, *Inorg. Chem.*, 2015, **54**, 12027−12031; (*b*) J. M. Zadrozny, J. Niklas, O. G. Poluektov and D. E. Freedman, *ACS Cent. Sci.*, 2015, **1**, 488−492.

S6 Gaussian 09, Revision B.01, M. J. Frisch, G. W. Trucks, H. B. Schlegel, G. E. Scuseria, M. A. Robb, J. R. Cheeseman, G.Scalmani, V. Barone, B. Mennucci, G. A. Petersson, H. Nakatsuji, M. Caricato, X. Li, H. P. Hratchian, A. F. Izmaylov, J. Bloino, G. Zheng, J. L. Sonnenberg, M. Hada, M. Ehara, K. Toyota, R. Fukuda, J. Hasegawa, M. Ishida, T. Nakajima, Y. Honda, O. Kitao, H. Nakai, T. Vreven, Jr. J. A. Montgomery, J. E. Peralta, F. Ogliaro, M. Bearpark, J. J. Heyd, E. Brothers, K. N. Kudin, V. N. Staroverov, T. Kieth, R. Kobayashi, J. Normand, K. Raghavachari, A. Rendell, J. C. Burant, S. S. Iyengar, J. Tomasi, M. Cossi, N. Rega, N. J. Millam, M. Klene, J. E. Knox, J. B. Cross, V. Bakken, C. Adamo, J. Jaramillo, R. Gomperts, R. E. Stratmann, O. Yazyev, A. J. Austin, R. Cammi, C. Pomelli, J. W. Ochterski, R. L. Martin, K. Morokuma, V. G. Zakrzewski, G. A. Voth, P. Salvador, J. J. Dannenberg, S. Dapprich, A. D. Daniels, Ö. Farkas, J. B. Foresman, J. V. Ortiz, J. Cioslowski and D. J. Fox, Gaussian, Inc., Wallingford CT, 2010.

S7 T. Saito, S. Nishihara, Y. Kataoka, Y. Nakanishi, T. Matsui, Y. Kitagawa, T. Kawakami, M. Okumura and K. Yamaguchi, *Chem. Phys. Lett.*, 2009, **483**, 168–171.

Author Contributions

S. T. performed the chemical experiments, recorded all spectroscopic and magnetic data, carried out the theoretical calculations, and wrote the manuscript. H. R. and Y. Z performed the X-ray diffraction studies. Z. H. and Y. S. participated in the discussion of the SQUID results. Y. S. helped revising the magnetic properties section. X. W. conceived the project and revised the manuscript. All authors discussed the results and manuscript.